# Photochemical & Photobiological Sciences

Accepted Manuscript


This is an *Accepted Manuscript*, which has been through the Royal Society of Chemistry peer review process and has been accepted for publication.

*Accepted Manuscripts* are published online shortly after acceptance, before technical editing, formatting and proof reading. Using this free service, authors can make their results available to the community, in citable form, before we publish the edited article. We will replace this *Accepted Manuscript* with the edited and formatted *Advance Article* as soon as it is available.

You can find more information about *Accepted Manuscripts* in the Information for Authors.

Please note that technical editing may introduce minor changes to the text and/or graphics, which may alter content. The journal's standard Terms & Conditions and the Ethical guidelines still apply. In no event shall the Royal Society of Chemistry be held responsible for any errors or omissions in this *Accepted Manuscript* or any consequences arising from the use of any information it contains.

ROYAL SOCIETY OF CHEMISTRY

www.rsc.org/pps

Photochemistry and Photobiological Sciences RSCPublishing

ARTICLE

# Deciphering PDT-induced inflammatory responses using real-time FDG-PET in a mouse tumour model

Cite this: DOI: 10.1039/x0xx00000x

Nicole Cauchon[a], Haroutioun M. Hasséssian[b,c], Eric Turcotte[a], Roger Lecomte[a] and Johan E. van Lier[a,1]

Received 00th January 2012,
Accepted 00th January 2012

DOI: 10.1039/x0xx00000x

www.rsc.org/

Dynamic positron emission tomography (PET), combined with constant infusion of 2-deoxy-2-[$^{18}$F]fluoro-D-glucose (FDG), enables real-time monitoring of transient metabolic changes in vivo, which can serve to understand the underlying physiology. Here we investigated characteristic changes in the tumour FDG-uptake profiles in relation to acute localized inflammatory responses induced by photodynamic therapy (PDT). Dynamic PET imaging with constant FDG infusion was used with EMT-6 tumour bearing mice. FDG time-activity uptake curves were measured simultaneously, in treated and reference tumours, for 3 h, before, during, and after PDT. Inflammation was studied when evoked by PDT using either a trisulfonated porphyrazine photosensitizer ($ZnNPS_3C_6$), or lipopolysaccharide (LPS), and inhibited using indomethacin. The distinct transient patterns, characterized by drops and subsequent recovery of tumour FDG uptake rates, were also analysed using immunohistochemical markers for apoptosis, necrosis, and inflammation. Typical profiles for tumour FDG-uptake, consisted of a drop during PDT, followed by a gradual recovery period. Tumours treated with LPS, but not with light, showed a continuous increase in FDG-uptake during the 3 h experimental period. Treatment with indomethacin, inhibited the rise in FDG-uptake observed with either LPS or PDT. Tumour FDG-uptake profiles correlated with necrosis markers during PDT, and inflammatory response markers post-PDT, but not with an apoptosis marker at any time during or after PDT. Dynamic FDG-PET imaging combined with indomethacin reveals that, the drop in the tumour FDG-uptake rate during the PDT illumination phase reflects vascular collapse and necrosis, while the increased tumour FDG-uptake rate immediately post-illumination involves an acute localized inflammatory response. Dynamic FDG infusion and PET imaging, combined with the use of selective inhibitors, provides unique insight for deciphering the complex underlying processes leading to tumour response in PDT, and allows for rapid as well as cost effective optimization of PDT protocols.

[1]Correspondence Professor J.E. van Lier; Email: Johan.E.vanlier@USherbrooke.ca

Photochemistry and Photobiological Sciences RSCPublishing

ARTICLE

## Introduction

Use of 2-deoxy-2-[$^{18}$F]fluoro-D-glucose (FDG) tracer is the most common (about 90%) type of positron emission tomography (PET) imaging in standard medical care for cancer. Therefore, being able to predict therapeutic outcome from tumour FDG-uptake profiles at the start of the treatment, will be a powerful tool, and very useful in treatment optimization protocols. Earlier, we demonstrated that different mechanisms of action correlate with real-time changes in the tumour FDG uptake profile, during photodynamic therapy (PDT), monitored by dynamic PET.[1] We showed that the FDG-uptake changes, which take place early in the PDT protocol, have predictive value for the outcome of the treatment.[2,3]

Induction of an acute localized inflammatory response is of benefit to PDT. It contributes to the antitumour effects of PDT, and helps to facilitate the development of a systemic immune response, which is of a longer time scale.[4,5] The acute localized inflammatory response requires constant stimulation to be sustained. It ceases once the stimulus is removed, since inflammatory mediators have short half-lives and are rapidly degraded in tissue. Understanding such acute localized inflammation, with the goal to control it, is of vital importance.[5]

Typically, FDG-PET imaging conducted concurrently with PDT showed a drop in tumour FDG-uptake rates during illumination, with a progressive increase in the FDG-uptake rates, toward recovery, post-illumination.[1] We also detected significant differences in the delay-to-response times ($\Delta_1$), which denotes the time required for PDT to affect the FDG-uptake rate, and the delay-to-recovery times ($\Delta_2$), which denotes the time required for recovery of the FDG-uptake rate post-illumination.[1] A short delay-to-response combined with a drop in the FDG uptake rate during illumination, indicates a major contribution by a direct cell kill pathway, such as induction of apoptosis and/or necrosis.[1] In contrast, a long delay-to-response, combined with a long delay-to-recovery, signifies cell death via predominantly an indirect cell kill pathway, such as damage to tumour vasculature, leading to oxygen starvation of cells.[1] A short delay-to-response together with a strong drop in the tumour FDG-uptake rate during illumination, followed by a complete recovery of the tumour FDG-uptake rate, corresponded to the greatest PDT efficacy, and best long-term tumour response outcome.[1] Thus, using FDG-PET imaging, within 60 min after start of the PDT protocol, it is possible to predict the long term tumour response outcome.

Recovery of the FDG-uptake rate, observed post-illumination, may result from metabolic activity induced in the tissue due to several possible factors.[6,7] These factors may include additional metabolic activity contributed by: 1) increased energy requirements of surviving tumour cells due to repair mechanisms, or cell death pathways,[8] and/or 2) gathering inflammatory cells.[9] One or a combination of such factors could explain the increase in the FDG-uptake rate observed in tumours post-illumination.[10,11]

The participation of prostaglandins (PGE2) and thromboxanes in post-illumination (post-PDT) inflammatory responses is well documented.[5,12] Non-steroidal anti-inflammatory drugs (NSAIDs) are widely used as inhibitors of inflammation. Among these drugs, indomethacin is used as a potent, non-specific, inhibitor of cyclooxygenase (COX) enzymes which metabolize arachidonic acid to PGE2, prostacyclins (PGI2), and thromboxanes.[13] Bacterial lipopolysaccharide (LPS), a well-known antigen,[14] triggers cell death and activates inflammation.[15] Studies have shown that LPS administration provokes a partial anti-tumour effect, although under these circumstances, complete tumour regression requires a systemic immune response.[16-18]

Our current study addresses the role of acute localized inflammation in hexynyl trisulfobenzo-mononaphtho-porphyrazine ($ZnNPS_3C_6$) based PDT[1,19] induced tumour response as monitored by real-time FDG-PET. We used immunohistochemistry (IHC) to evaluate the role of specific inflammatory mediators immediately post-illumination, and pharmacology to evaluate their role in correlation with the increased tumour FDG-uptake rate.

## Materials and Methods

### Photosensitizer

All solutions were prepared with ultra-pure water (>18.0 MΩ cm resistivity). About 10 mg of photosensitizer $ZnNPS_3C_6$,[1,19] was formulated in 1% PBS (3 mL), sonicated for a few minutes, and filtered over a 0.22-μm filter (Millipore). The final concentration of the photosensitizer was adjusted with 1% PBS to 100 μM after determining the concentration by UV-Vis spectroscopy of a 50-fold diluted sample in methanol.

### Cell cultures

The EMT-6 murine mammary tumour cell line was maintained in Waymouth MB 752/1 medium culture (Sigma-Aldrich, St Louis, MO, USA) supplemented with 15% foetal bovine serum (FBS), 1% glutamine and 1% pen-strep (Gibco, Burlington, ON, Canada).

**Animal model**

The experiments were conducted in accordance with protocols approved by the Canadian Council on Animal Care, and the Université de Sherbrooke Ethics Committee. Animals were allowed free access to water and food during the progression of the experiments. All experiments were performed on Balb/c female mice (19-21 g) (Charles River Breeding Laboratories). Before tumour implantation, hair on the hind legs, and the back of the animals, was removed by shaving and epilating. The two tumours were introduced approximately 1.8 cm from each other on the back of the animals, by i.d. injection of 2-3 × $10^5$ EMT-6 cells, suspended in 0.05 mL Waymouth growth medium.

**Photodynamic therapy**

The PDT protocol was similar to what was previously described.[1] Briefly, one week after tumour implantation, when tumour diameters had reached 5-8 mm (2-3 mm thick), animals received photosensitizer ($ZnNPS_3C_6$, 1 μmol.kg$^{-1}$, i.v.) or PBS, followed 24 h later by 670±10 nm diode laser-light treatment (model BWF-670-300, D&W TEK, Newark, DE, USA) of one tumour. The companion tumour was shielded from light and served as a reference. The light beam (~8 mm, 200 mW.cm$^{-2}$) was spread uniformly over the whole tumour area. The light delivery was applied cyclically: 5 min illumination followed by 2 min dark. The illumination time was spread over 40 min. Taking into account the dark periods, a total fluence of 365 J.cm$^{-2}$ was delivered.

**Induction and/or inhibition of inflammation**

Animals were divided into five groups. One group of mice, received intratumoural 50 μL of LPS (5 mg.ml$^{-1}$) in one tumour 30 sec prior to imaging, to activate localised inflammation, and did not receive PDT. The second group, received i.v. 0.1 mL indomethacin (2 mg.kg$^{-1}$), 30 sec prior to imaging, after which PDT started 30 min later. The third group received both indomethacin and LPS within 30 sec prior to imaging, without PDT. The fourth group received only PDT. The fifth group of animals received no treatment.

**Radiopharmaceuticals**

Fluorine-18 was prepared by the $^{18}O$ (*p*,*n*) $^{18}F$ reaction on $^{18}O$-enriched water as target material using a TR-19 cyclotron (Advanced Cyclotron Systems Inc., Richmond, BC, Canada). FDG was prepared on site following established procedures.[20] FDG activity was measured with a CRC-35R dose calibrator (Capintec, Ramsey, NJ, USA).

**PET imaging**

PET was performed using a LabPET™ (Gamma Medica, Sherbrooke, QC, Canada) small animal scanner, with a 3.75 cm axial field of view, and a transaxial resolution of 1.35 mm FWHM (full width at half-maximum peak height) (Bergeron et al., 2009).[21] The mice were anesthetized (2.5% isoflurane in medical $O_2$), and a butterfly needle-30G1/2 was placed in the tail vein. After fixing the cannula, mice received indomethacin or LPS, depending on the group selected, and were then placed supine on the temperature regulated heating bed of the camera. The position of the scanner bed was adjusted in order to place the tumours, with the help of a laser pointer, at the center of the axial field of view. A 3 h dynamic PET image acquisition was then launched. After a 30 sec delay, the mice were continuously infused with FDG (70-80 MBq in 1 mL of 0.9% NaCl at 0.003 mL/min). For animals receiving PDT, the treated tumour was exposed to red light from the laser diode 30 min after starting FDG infusion. PET imaging was then continued for about 2 h more, to complete the total 3 h scan sequence. The vital signs of the animals were monitored and recorded throughout the 3 h imaging period to ensure a stable physiology at all times. Three or four mice were scanned for each group. To get a more accurate measure of the injected FDG dose, the radioactivity in each animal was quantified in a well counter at the end of imaging, and the mice were then euthanized.

**Image Analysis**

The images were reconstructed using 10, 15, and 20 iterations, of a 2D maximum likelihood expectation maximization (ML-EM) algorithm, which models detector response. Overall, 31 images in 128 × 128 pixels format (voxel size of 0.50 × 0.50 × 1.19 mm$^3$) were obtained axially, covering 37 mm of tissue. PET image series consisted of 90 frames of 120 s. Regions of interest (ROI) were traced over the reference and treated tumours, on the last frame of the dynamic image series, and applied to all preceding frames. Radioactive decay corrected FDG-uptake curves were generated, and analysed according to a previously described mathematical model.[1,2] The PET images were analysed with the Sherbrooke LabPET software (Université de Sherbrooke, Sherbrooke, QC, Canada). Kinetic analysis and curve-fitting were performed using the GraphPad Prism software (GraphPad Software Inc., San Diego, CA, USA).

**Immunohistochemical analysis (IHC)**

Briefly, EMT-6 tumour bearing mice were injected through the caudal vein with PBS or indomethacin, and 30 min later, mice were treated with PDT or LPS as described above. Tumours were excised, washed with PBS, and fixed with 2% buffered formaldehyde; immediately, 1, 2 and 3 h after PDT, or 3 h after LPS injection. After a 24 h fixation period, tumours were embedded in paraffin for sectioning. Paraffin embedded histological sections (5 μm) were sectioned with a microtome, mounted on silanized slides (in duplicate), dewaxed in xylene, and rehydrated through graded alcohols. An additional set of sections, which served as negative controls, were treated similarly, but without the primary antibody. Other sections, known to react with antibody, were used as positive controls. First, antigen retrieval was performed by heat treatment in citrate buffer for 30 min, using a vegetable steamer. After blocking overnight with 20% BSA, sections were incubated 2

h at room temperature, with the following primary antibodies, directed against the following proteins: Annexin V (1:100; Santa Cruz Biotechnology, USA, CA), and PMN directed against rat neutrophils (1:100, Cedarlane, Canada, ON). For macrophage detection, sections were incubated 2 h at room temperature with IBA 1 (1:100; Wako Chemical USA, VA) without the blocking step. The appropriate HRP-conjugated secondary antibody (goat anti-rabbit; sc-2004 from Santa Cruz Biotechnology, USA, CA) was used for each primary antibody, and incubated for 1 h at room temperature. Labeling was revealed using diaminobenzidene (DAB) (Roche, QC, Canada). Slides were counterstained with hematoxylin. Slides were dehydrated through graded alcohols, cleared with xylene, and cover-slipped using Permount mounting media (Fisher Scientific, Canada, ON).[22]

All slides were analysed using light microscopy under either 400X or 600X magnification. Staining intensities of each slide (6-8 fields) were quantified using the Image J program (NIH, USA), and thus used to quantify the response.[23] Although IHC may be less sensitive than Western blotting, the advantage of IHC is that it allows observation of intact tissues, and this without extraction or digestion procedures. With IHC, the detection of a given antigen, provides a reliable basis for comparisons between tissues that are treated with the same experimental conditions.

### Data analysis

Data are presented as mean ± standard error of the mean (SEM) taken from 3-4 animals. Comparisons between different conditions were performed using analysis of variance (ANOVA) with Tukey's multiple comparisons test. A probability of $P \leq 0.05$ was considered statistically significant. Due to multiple comparisons, and for the purpose of clarity, we have given the degree of statistical significance in the legend to the figure, as opposed to labels (such as asterisk), directly on the graphs or within the tables.

## Results

### Response to LPS and inhibition by Indomethacin

Table 1. FDG tumour uptake rates after LPS injection, with and without Indomethacin, over a 3h period.

| | FDG-uptake rates [a] (count/pixel/min) |
|---|---|
| Reference | 5.48 ± 0.19 |
| LPS | 7.51 ± 0.15 |
| LPS + Indomethacin | 4.43 ± 0.22 |

[a] The average FDG tumour uptake rates during a 3h infusion are expressed relative to the total amount of FDG at the end of the scan (Cauchon et al, 2012). Probability values P are, LPS vs Reference: P<0.0001, LPS + Indomethacin vs Reference: P<0.01, LPS vs. LPS + Indomethacin: P<0.0001.

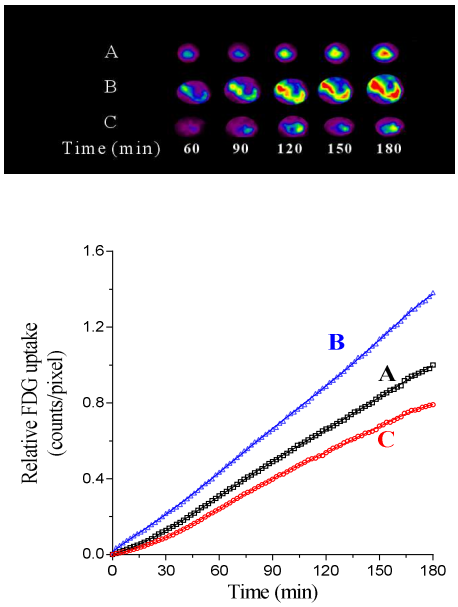


Fig. 1 Effect of LPS and Indomethacin on tumour FDG-uptake during a 3 h period. Top panel: PET scans showing FDG uptake in transaxial slices of LPS treated and reference tumours, with and without Indomethacin, at different time intervals after the start of FDG infusion. (A) Reference tumour; (B): Tumour directly injected with LPS; (C) LPS-treated animals which received Indomethacin (i.v.) 30 s prior to starting the PET scan. Lower panel: corresponding FDG uptake curves generated from such tumours during a 3 h period. Probability values are: LPS (B, blue) vs Reference (A, black), P<0.0001; LPS + Indomethacin (C, red) vs Reference (A, black), P<0.01; LPS (B, blue) vs LPS + Indomethacin (C, red), P<0.0001.

Over the 3 h scanning period, a progressive increase in tumour FDG-uptake was visible on the PET scans immediately after LPS injection (Fig. 1: top panel), and the corresponding curves of FDG uptake in relation to time (Fig. 1: lower panel) were derived from the PET scans.

Compared to the reference tumour, treatment with LPS resulted in a 40% increase in the FDG-uptake rate (Table 1), and a 37% higher total tumour FDG accumulation at the end of the scan. Pre-administration of indomethacin to LPS treated mice, caused a reduction of about 50% in the FDG-uptake rate when compared to animals which received LPS but no indomethacin (Fig. 1; lower panel and Table 1). Administration of indomethacin alone had no significant effect on the tumour FDG-uptake rate (data not shown).

Immunostaining of tumours excised 3 h after LPS injection, revealed an increase in activated macrophages, and partial induction of cell death (Fig. 2). Pre-administration of indomethacin to LPS treated mice strongly inhibited macrophage activation, and partially reduced PMN expression, but had no significant effect on cell death (Fig. 2).

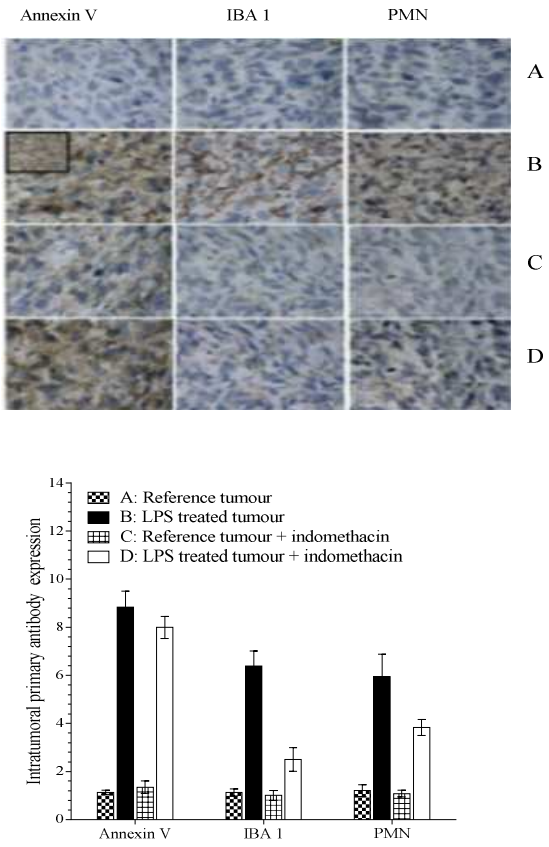


Fig. 2. Immunohistochemistry (IHC) of LPS and/or Indomethacin treated tumours. Tumours were excised 3 h post LPS and/or Indomethacin treatment, and stained with Annexin-V (cell death marker), IBA 1 (marker for activated macrophages), or PMN (polymorphonuclear leucocytes). Top panel shows immunohistochemical slides, and lower panel shows corresponding staining intensities relative to untreated tumour tissue (6-8 fields) presented as bar plots. For comparison of the difference between LPS vs Reference, a P<0.0001 was measured for antigens (Annexin-V, IBA 1, PMN). For LPS + Indomethacin vs Reference, a P<0.001 was measured for antigens (Annexin-V, ABA 1, PMN). In contrast, for LPS vs LPS + Indomethacin, a statistically significant difference (P<0.001) was found for only IBA 1 and for PMN.

## Tumour response to PDT and effect of Indomethacin

Table 2. FDG-uptake rates before, during and after PDT, with and without Indomethacin, over a 3h period.

| | FDG-uptake rates [a] (counts/pixel/min) | | |
|---|---|---|---|
| | $m_1$ | $m_2$ | $m_3$ |
| Reference | 4.92 ± 0.14 | 6.46 ± 0.05 | 5.47 ± 0.02 |
| PDT | 4.83 ± 0.11 | 4.04 ± 0.07 | 4.79 ± 0.03 |
| PDT + Indomethacin | 5.01 ± 0.20 | 6.08 ± 0.19 | 3.02 ± 0.04 |

[a] The FDG uptake-rates before ($m_1$), during ($m_2$) and after PDT ($m_3$) are expressed relative to total FDG at the end of each 3 h scan and calculated from FDG uptake curves presented in Fig. 4. No significant (P>0.05) difference was detected between the $m_1$ values of reference, PDT or PDT + Indomethacin. A significant difference was detected for $m_2$ values as follows: PDT vs reference (P<0.0001), and PDT vs PDT + Indomethacin (P<0.0001). Among $m_3$ values, a significant (P<0.01) difference was detected between reference vs PDT, as well as between PDT vs PDT + Indomethacin (P<0.0001).

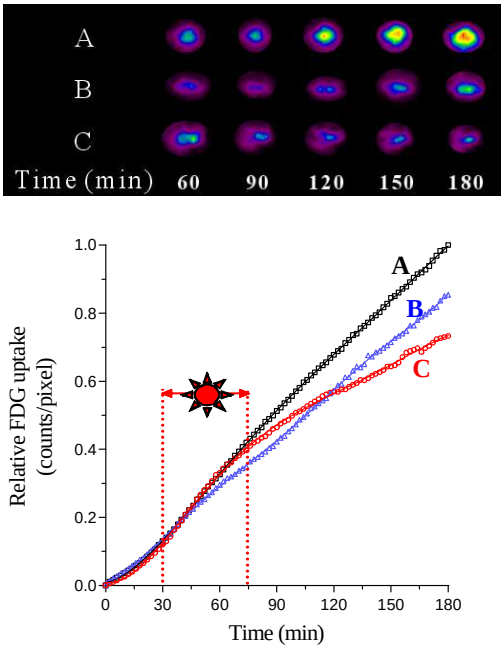


Fig. 3. Effect of Indomethacin on tumour FDG-uptake during PDT. Top panel: PET scans showing FDG uptake in transaxial slices of Reference tumours, and of $ZnNPS_3C_6$-PDT treated tumours, at different time intervals after the start of FDG infusion. Lower panel: FDG uptake curves generated over tumours during a 3 h period. (A) Reference tumour, no light (Black); (B) Light-treated tumour (Blue); (C) Light-treated tumour of animals which received Indomethacin (i.v.) 30 s prior to starting the PET scan (Red). : Probability values were: PDT (B, blue) vs Reference (A, black), P<0.001; PDT + Indomethacin (C, red) vs Reference (A, black), P<0.0001; PDT (B, blue) vs PDT + Indomethacin (C, red), P<0.01.

Over the 3 h scanning period, changes in tumour FDG-uptake immediately after PDT, with and without indomethacin, are visible on the PET scans (Fig. 3, top panel), and on the corresponding FDG-uptake curves (Fig. 3, lower panel). From these curves the FDG-uptake rates before ($m_1$), during ($m_2$), and after ($m_3$) PDT, were calculated (Table 2), as well as the percent change in the rates (Fig. 4). Delay-to-response ($\Delta_1$) and delay-to-recovery ($\Delta_2$) times were also estimated from the tumour FDG-uptake curves (Fig. 5).

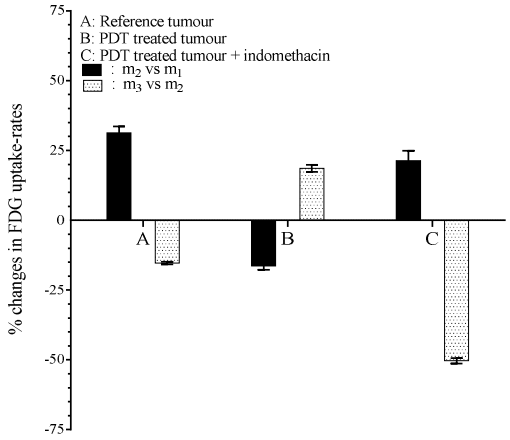


Fig. 4. Percent change in tumour FDG-uptake rates as a result of PDT (derived from Table 2). Probability values during illumination were: PDT + Indomethacin vs Reference, P<0.01; PDT vs PDT + Indomethacin, P<0.0001. Probability values after illumination were: P<0.0001 for PDT vs Reference, for PDT + Indomethacin vs Reference, and for PDT vs PDT + Indomethacin.

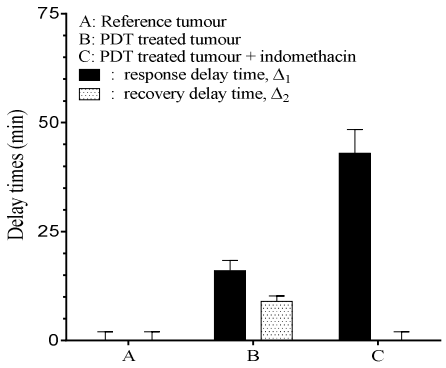


Fig. 5. Delay times affecting FDG uptake-rates during and after PDT (derived from Fig. 3). (A) Reference tumour; (B) PDT treated tumour without Indomethacin; (C) PDT treated tumour with Indomethacin. Probability values for $\Delta_1$ were as follows: PDT vs Reference, P<0.01; PDT + Indomethacin vs Reference or PDT, P<0.0001. Probability values for $\Delta_2$ were as follows: PDT vs Reference or PDT + Indomethacin, P<0.05.

For PDT treated mice, the FDG-uptake rate decreased after a 16 min delay-to-response ($\Delta_1$), and showed a 9 min delay-to-recovery ($\Delta_2$) (Fig. 5). Pre-administration of indomethacin prior to PDT caused a significant change in the FDG-uptake profile, such that during the light-on period there was an increase in the tumour FDG-uptake rate (Table 2). In contrast, immediately post-illumination ($m_3$) a strong decrease in the uptake rate, relative to $m_1$ or $m_2$, was observed in the group pre-administered indomethacin (Table 2). Over the 3 h period, the total tumour FDG-uptake was reduced by about 12% following treatment with indomethacin, which amounted to a 30% reduction when compared to the reference tumour (Fig. 3). Treatment with indomethacin also had a significant effect on the delay times (Fig. 5). A change in the FDG-uptake rate (delay-to-response, $\Delta_1$) was increased to about 43 min, whereas the delay-to-recovery ($\Delta_2$) was reduced to near zero (Fig. 5). Thus in the presence of indomethacin, the drop in FDG-uptake which normally occurs during PDT ($m_2$) did not take place (Fig. 4 and Table 2). Instead there was a drop in FDG-uptake post-illumination ($m_3$) which was very short lasting (Fig. 4 and Table 2).

To correlate these changes in tumour FDG-uptake rates to possible cellular and molecular responses which mediate acute localized inflammation, we analysed the treated and reference tumours at various times (0-3 h) post-PDT, using immunohistochemistry (Fig. 6). These data show that PDT activated macrophages immediately post-illumination, and macrophage levels returned to baseline by 2 h (Fig. 6A). In contrast, although PMN expression increased immediately post-illumination, it remained high, up to 2 h after PDT (Fig. 6B). Annexin V expression (cell death) reached a maximum at the last observation point (3 h post-PDT) (Fig. 6C). Pre-administration of indomethacin prior to PDT blocked expression of all three selected immunohistochemistry markers (Fig. 6).

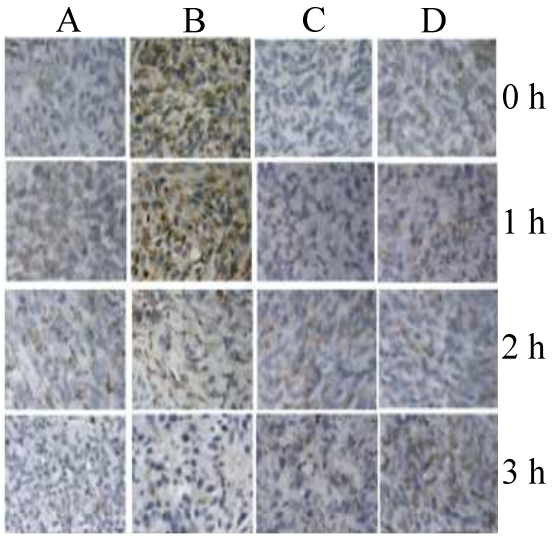


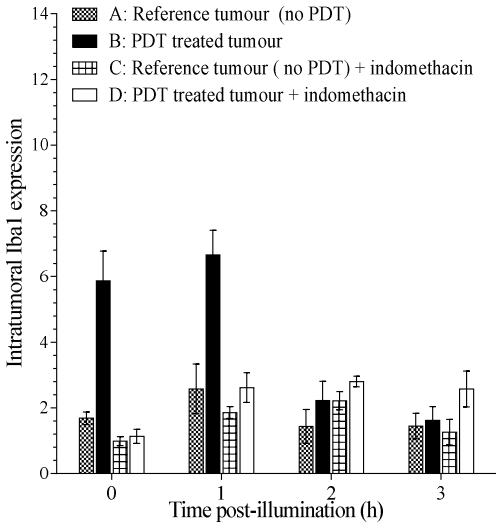


Fig. 6A. Immunohistochemistry (IHC) of PDT treated and Reference tumours. Tumours were excised 0-3 h post-PDT and stained with IBA 1. Staining intensities relative to untreated EMT-6 tumour tissue (6-8 fields) are presented as bar plots. A probability of P<0.0001 was calculated for PDT vs Reference; or for PDT vs Reference + Indomethacin, or for PDT + Indomethacin after 0 and 1 h post illumination.

.

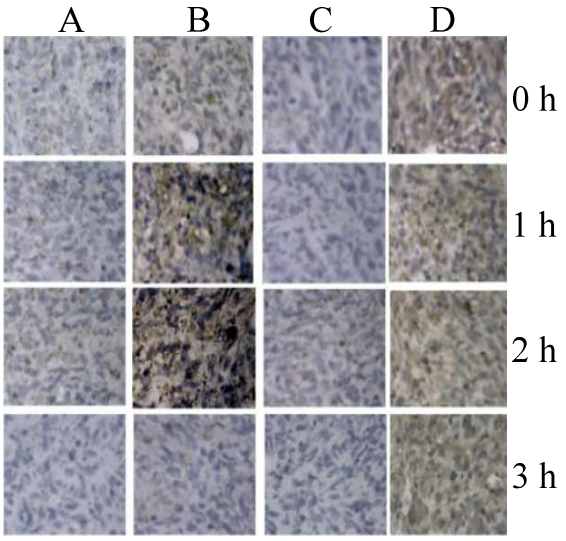


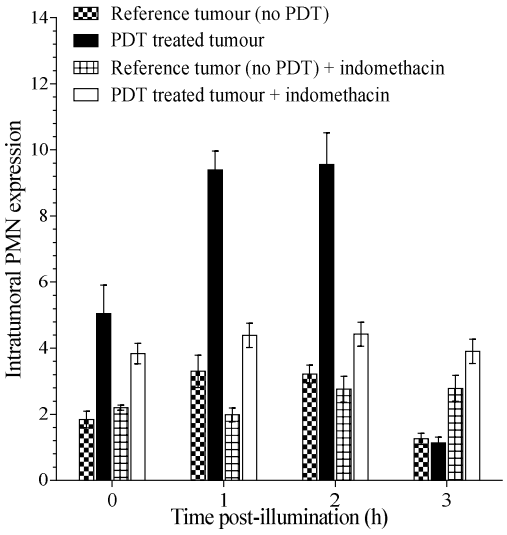


Fig. 6B. Immunohistochemistry (IHC) of PDT treated and Reference tumours. Tumours were excised 0-3 h post-PDT and stained with PMN. Staining intensities relative to untreated EMT-6 tumour tissue (6-8 fields) are presented as bar plots. Probability values were as follows: PDT vs Reference, or for Reference + Indomethacin, or PDT + Indomethacin, P<0.0001 (1 and 2 h); PDT vs Reference, or Reference + Indomethacin, P<0.001 (0 h), PDT + Indomethacin vs Reference + Indomethacin, P<0.05 (1 h and 2 h) and PDT + Indomethacin vs Reference or PDT, P<0.01 (3 h).

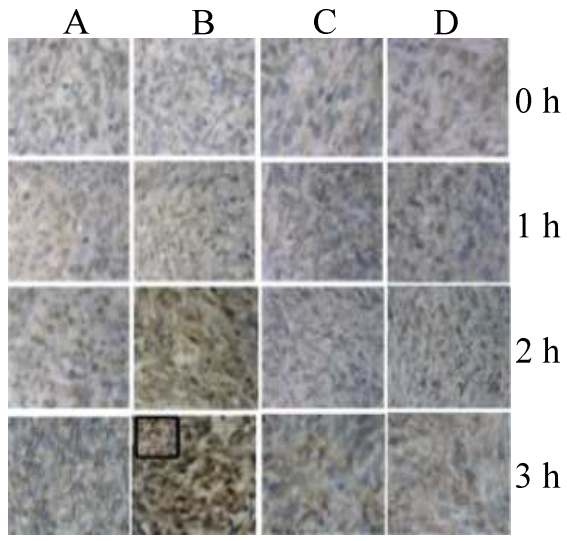


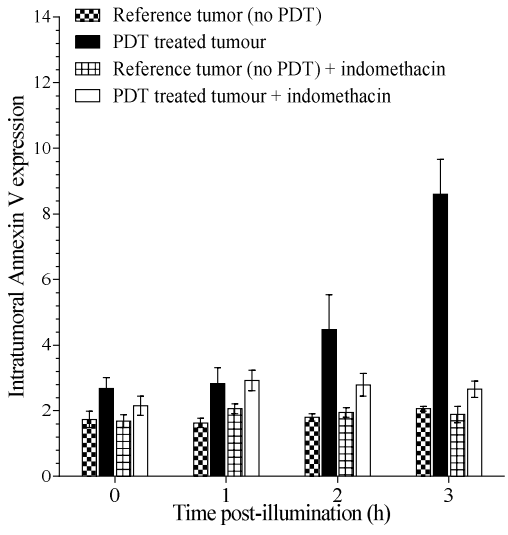


Fig. 6C. Immunohistochemistry (IHC) of PDT treated and Reference tumours. Tumours were excised 0-3 h post-PDT and stained with Annexin v. Staining intensities relative to untreated EMT-6 tumour tissue (6-8 fields) are presented as bar plots. Probability values were as follows: PDT vs Reference; Reference + Indomethacin, or vs PDT + Indomethacin, P<0.0001 (3 h); PDT vs Reference or Reference + Indomethacin, P<0.01 (2 h), and PDT vs PDT + Indomethacin, P<0.05 (2 h).

## Discussion

In the laboratory and the clinic, PET imaging is a quantifiable tool used in standard diagnostic nuclear medicine.[1,2,23] Among various radiotracers used for this purpose, FDG is the most prominent, since it allows detection of metabolic activity, delineation of tumours and their metastases, as well as follow-up to therapeutic intervention. A decrease in tumour FDG-uptake usually correlates directly with cell inactivation, and/or reduced blood flow due to vascular collapse.[1,2,24] In contrast, an increase in FDG-uptake reflects augmented metabolic activity, which may be related to activation of cell-death pathways, cell proliferation, or inflammation.[2,7,25]

Among the various photosensitizers which we have evaluated in this model, we found that the newly developed amphiphilic porphyrazine ($ZnNPS_3C_6$), together with a fractionated light treatment protocol, exerted the most dramatic effect on the tumour FDG-uptake rate.[1,19] The FDG-uptake profile associated with $ZnNPS_3C_6$-PDT was characterized by: a short delay-to-response ($\Delta_1$), a decrease in tumour FDG-uptake during illumination ($m_2$), followed by a strong recovery post-illumination ($m_3$).[1] We concluded that this response profile involved both direct as well as indirect cell kill pathways, and that inflammatory mediators are involved in both pathways.

Due to such a central role of inflammation, in the current study, we evaluated a possible correlation between the observed changes in tumour FDG-uptake rates and tumour immune responses, during and shortly after light-fractionated PDT with $ZnNPS_3C_6$. The current study showed that acute localized inflammation induced by this PDT protocol correlates with the post-illumination tumour FDG-uptake response. Late (beyond 3 h) systemic immune responses, which may be activated, fall outside of the time-scale of our current study.

Non-steroidal anti-inflammatory drugs, such as indomethacin, produce their effects through the inhibition of COX isoenzymes, of which three variants are known to exist.[26,27] COX-1 is considered to be a constitutive enzyme, whereas COX-2 is an inducible enzyme, whose levels increase in activated macrophages, and other cells at sites of inflammation.[26,28] COX-2 has also been shown to be up-regulated in various carcinomas,[29,30] and to have an important role in tumourigenesis.[31,32] COX-3 is a splice variant of COX-1.[26] Indomethacin is a potent inhibitor of all three COX isoenzymes.[26] The COX isoenzymes act on arachidonic acid (AA), and are responsible for the production of Series-2 prostanoids.[33] Series-1 and Series-3 protanoids are also derived from COX activity, through oxygenation of di-homo-gamma-linolenic acid (DGLA) and eicosapentaenoic acid (EPA). However, Series-1 and Series-3 prostanoids are less inflammatory than Series-2 prostanoids.[33]

Using an air pouch inflammation model, Kamachi et al. showed that oral administration of indomethacin ($\geq 0.01$ μM) to mice, inhibits LPS-induced production of PGE2, and no concurrent infiltration of leukocytes was detected.[34] A similar inhibition by indomethacin of PDT-induced inflammation has previously been reported.[35,36] However, the role of PGE2 in PDT remains controversial. Both an increase and a reduction in tumour cell sensitivity, following inhibition of PGE2 synthesis, have been observed.[13,37] This discrepancy can be attributed to differences in tissue COX levels, competitive inhibition of COX by DGLA or EPA, and possible involvement of other AA metabolizing enzymes, as well as variations in PDT protocols. Nevertheless, it is clear that PGE2 mediate inflammation, and that there is acute localized inflammation following PDT.

To establish that our FDG-PET imaging protocol can detect acute localized inflammation, we used direct injection of LPS into tumour tissue. The resulting FDG-uptake profile was characterized by a rapid, and almost linear, 30% increase in the FDG-uptake rate when compared to the reference tumour (Fig. 2; Table 1). Pre-administration of indomethacin, inhibited the LPS-induced effect, suggesting that the increase in tumour FDG-uptake rate corresponds to a cyclooxygenase mediated inflammatory response. In addition, we observed that compared to the FDG-uptake in the reference tumour, the indomethacin treated animals showed a 20% decrease in total tumour FDG-uptake, which likely represents inhibition of tumour associated inflammation.

We found that, contrary to LPS induced inflammation, the response to $ZnNPS_3C_6$-PDT involved both activation of inflammatory mediators and vascular effects. Macrophages are normally present in all tissues, including tumours, and initiate the process of acute localized inflammation. However, leukocytes which normally circulate in blood, move into the inflamed tissue via extravasation. Macrophages, leukocytes, and other cells which mediate inflammation, release substances which develop and maintain the inflammatory response. The extent of apoptosis, necrosis and inflammatory cell invasion was evaluated by immunohistochemistry in our current study. Annexin V was selected for the detection of cell death, including apoptosis and necrosis. IBA1 is a 17-kDa EF hand protein that is specifically expressed in macrophages/microglia and is up regulated during the activation of these cells. The presence of polymorphonuclear leukocytes (PMN) inside tumours was estimated using an antiserum directed against rat PMNs. LPS treated tumours showed a dramatic increase in the concentration of all three immuno markers (Annexin V, IBA 1 and PMN) (Fig. 3). When treated with indomethacin, we observed a decrease in IBA 1 and PMN, but no effect on Annexin V expression in LPS-treated tumours. These results show that indomethacin inhibited inflammation but not apoptosis. In tumours not treated with LPS or PDT, these immuno-markers were not affected by treatment with indomethacin. This shows that indomethacin does not have an effect on baseline levels of these immuno-markers.

The effects of $ZnNPS_3C_6$-PDT on tumour FDG-uptake were twofold (Fig. 4): first, during illumination, the uptake rate started to decrease 16 min after the start of illumination (delay-to-response, $\Delta_1$), and second, 9 min post-illumination (delay-to-recovery, $\Delta_2$) recovered to the same rate observed prior to PDT (Table 2). Immunostaining of PDT exposed tumour tissue, showed immediate macrophage activation, followed by invasion with PMN, and subsequently a progressive increase in Annexin V expression (Fig. 6). Hence, $ZnNPS_3C_6$ based PDT evokes acute localized inflammation, and later activates necrosis. The rapid acute localized inflammatory response to PDT was evident from the early response of PMN and macrophages.

Indomethacin administration prior to PDT clearly affected the tumour FDG-uptake profile. During the illumination phase ($m_2$), the FDG-uptake rate, rather than being depressed, in fact increased, compared to the reference tumour (Figure 4 and Table 2). The augmented FDG-uptake rate during PDT is likely due to a facilitation of vasodilation brought about by treatment with indomethacin.[38,39] It was more than 40 min after the start of illumination that the tumour FDG-uptake rate decreased significantly. The effect of indomethacin on the PDT tumour response is particularly evident when looking at the percent change in tumour FDG-uptake rates during $[(m_2-m_1)/m_1]$ and after $[(m_3-m_2)/m_2]$ PDT (Fig. 5). This reveals that administration of indomethacin prior to PDT inverses the FDG uptake pattern to yield a profile similar to that of the reference tumour, but with a pronounced diminution of the FDG-uptake rate after PDT. These data are in accord with our immunohistochemical data (Fig. 6), which confirm that indomethacin blocks the inflammatory response during the 2 h post-PDT. Furthermore, indomethacin prolongs the delay-to-response ($\Delta_1$) time four-fold (Fig. 6), suggesting a delayed indirect cell kill brought about by vascular collapse.[2,1] This delayed cell kill effect was confirmed by immunohistochemical staining, which clearly showed that apoptosis can only be detected 2 h post-PDT (Fig. 6). Thus, we interpret this to mean that the recovery of the tumour FDG-uptake rate immediately after PDT does not reflect apoptosis, but rather involves an acute localized inflammatory response. Such FDG-PET imaging as we used here, combined with the use of selective inhibitors, allow for the rapid detection of inflammation, and prediction of long term tumour response to the PDT protocol from events within the first 60 min. An added appeal of this approach is the need for fewer animals than conventional methods to monitor a PDT response.

## Conclusions

This is the first time IHC has been used to demonstrate specific mediators of inflammation correlated with the tumour FDG-uptake response to PDT. Using a pharmacological approach, we provided direct evidence for the participation of mediators in specific components of the FDG-uptake response to PDT. Our study shows the power of FDG-uptake imaging to quickly, and in a cost effective way, serve in the optimization of treatment protocols.

## Acknowledgements

This work was supported by the Jeanne and J.-Louis Lévesque Chair in Radiobiology (JEvL), and the Canadian Institutes of Health Research (PRG-80137, RL). JEvL, ET and RL are members of the Fonds de la Recherche en Santé du Québec-supported CRCHUS, Sherbrooke, QC, Canada. The authors are grateful to Marie-Elsa Brochu and Jean-François Beaudoin for their technical expertise.

## Notes and references

[a] Sherbrooke Molecular Imaging Centre, CRCHUS, and Department of Nuclear Medicine and Radiobiology, Université de Sherbrooke, Sherbrooke, QC, Canada J1H 5N4.
[b] Departments of Ophthalmology and Biomedical Sciences, Université de Montréal, Centre de Recherche Guy-Bernier, Hôpital Maisonneuve-Rosemont, 5415 Boul. de l'Assomption, Montréal, QC, Canada H1T 2M4.
[c] Present address: NorVision Therapeutics Inc, 1 Place Ville-Marie, Montréal, Québec, Canada H3B 2C4.

1. N. Cauchon, E. Turcotte, R. Lecomte, H. M. Hasséssian and J. E. van Lier. Predicting efficacy of photodynamic therapy by real-time FDG-PET in a mouse tumour model. *Photochem. Photobiol. Sci.*, 2012, 11, 364-370.
2. V. Bérard, J. A. Rousseau, J. Cadorette, L. Hubert, M. Bentourkia, J. E. van Lier, R. Lecomte. Dynamic imaging of transient metabolic processes by small-animal PET for the evaluation of photosensitizers in photodynamic therapy of cancer. *J. Nucl. Med.*, 2006, 47, 1119-1126.
3. A. T. Byrne, A. E. O'Connor, M. Hall, J. Murtagh, K. O'Neill, K. M. Curran, K. Mongrain, J. A. Rousseau, R. Lecomte, S. McGee, J. J. Calanan, D. F. O'Shea, W. M. Gallagher. Vascular-targeted photodynamic therapy with BF2-chelated Tetraaryl-Azadipyrromethene agents: a multi-modality molecular imaging approach to therapeutic assessment. *Br. J. Cancer*, 2009, 101, 1565-1573.
4. M. Koberlik. PDT-associated host response and its role in the therapy outcome. *Laser Surg. Med.*, 2006, 38, 500-508.
5. M. Firczuk, D. Nowisa, J. Goła. PDT-induced inflammatory and host responses. *Photochem. Photobiol. Sci.*, 2011, 10, 653-663.
6. N.L. Oleinick, R. Morris, I. Belichenko. The role of apoptosis in response to photodynamic therapy: what, where, why, and how. *Photochem. Photobiol. Sci.*, 2002, 1, 1-21.
7. N. Cauchon, R. Langlois, J. A. Rousseau, G. Tessier, J. Cadorette, R. Lecomte, D. J. Hunting, R. A. Pavan, S. K. Zeisler, J. E. van Lier. PET imaging of apoptosis with 64Cu-labeled streptavidin following

pretargeting of phosphatidylserine with biotinylated annexin-V. Eur. *J. Nucl. Med. Mol. Imaging*, 2007, 34, 247-258.

8. C. B. Oberdanner, T. Kiesslich, B. Krammer, K. Plaetzer. Glucose is required to maintain high ATP levels for the energy utilizing steps during PDT-induced apoptosis. *Photochem. Photobiol.*, 2002, 76, 695-703.
9. A. van Waarde, P. H. Elsinga. Proliferation markers for the differential diagnosis of tumour and inflammation. *Curr. Pharm. Design*, 2008, 14, 3326-3339.
10. A. P. Castano, P. Mroz, M. R. Hamblin. Photodynamic therapy and anti-tumour immunity. *Nat. Rev. Cancer*, 2006, 6, 535-545.
11. R. Kubota, S. Yamamda, K. Kubota, K. Ishiwata, N. Tamahashi, T. Ido. Intratumoural distribution of fluorin-18-fluorodeosyglucose in vivo; high accumulation in macrophages and granulation tissues studied by microauto-radiography. *J. Nucl. Med.*, 1992, 33, 1972-1980.
12. V. H. Fingar, T. J. Wieman, K. W. Doak. Role of thromboxane and prostacyclin release on photodynamic therapy-induced tumour destruction. *Cancer Res.*, 1990, 50, 2599-2603.
13. J. Kleban, J. Mikes, B. Szilardiova, J. Koval, V. Sackova, P. Solar. Modulation of hypericin photodynamic therapy by pretreatment with various inhibitors of arachidonic acid metabolism in colon adenocarcinoma HT-29 cells. *Photochem. Photobiol.*, 2007, 83, 1174-1185.
14. M. Fujiharaa, M. Muroib, K. I. Tanamotob, T. Suzukic, H. Azumaa, H. Ikedaa. Molecular mechanisms of macrophage activation and deactivation by lipopolysaccharide: roles of the receptor complex. *Pharmacol. Therapeut.*, 2003, 100, 171-194.
15. S. Nagano, T. Otsuka, H. Niiro, K. Yamaoka, Y. Arinobu, E. Ogami, M. Akahoshi, Y. Inoue, K. Miyake, H. Nakashima, Y. Niho, M. Harada. Molecular mechanisms of lipopolysaccharide-induced cyclooxygenase-2 expression in human neutrophils: involvement of the mitogen-activated protein kinase pathway and regulation by anti-inflammatory cytokines. *Int. Immunol.*, 2002, 14, 733-740.
16. W. G. Bessler, K. Mittenbühler, U. Esche, M. Huber. Lipopeptide adjuvants in combination treatment. *Int. Immunopharmacol.*, 2003, 3, 1217-1224.
17. M. R. Chicoine, M. Zahner, E. K. Won, R. R. Kalra, T. Kitamura, A. Perry, R. Higashikubo. The in vivo antitumoural effects of lipopolysaccharide against glioblastoma multiforme are mediated in part by Toll-like receptor 4. *Neurosurgery*, 2007, 60, 372-381.
18. S. Basith, B. Manavalan, G. Lee, S. Geon Kim, S. Choi. Toll-like receptor modulators: a patent review (2006-2010). *Expert Opin. Ther. Pat.*, 2011, 21, 927-944.
19. J.E. van Lier, H. Tian, H. Ali, N. Cauchon, H. M. Hasséssian. Trisulfonated porphyrazines: new photosensitizers for the treatment of retinal and sub-retinal oedema. *J. Med. Chem.*, 2009, 52, 4107-4110.
20. K. Hamacher, H. H. Coenen, G. Stocklin. Efficient stereo-specific synthesis of no-carrier-added 2-[18F]-fluoro-2-deoxy-D-glucose using aminopolyether supported nucleophilic substitution. J. Nucl. Med., 1986, 27, 235–238.
21. M. Bergeron, J. Cadorette, J. F. Beaudoin, M. D. Lepage, G. Robert, V. Selivanov, M. A. Tétrault, N. Viscogliosi, J.P. Noremberg, R .Fontaine, R. Lecomte. Performance evaluation of the LabPET™ APD-based digital PET scanner. IEEE Trans. Nucl. Sci., 2009, 56, 10-16.
22. S. Girard, G. Sébire, H. Kadhim, Proinflammatory orientation of the interleukin 1 system and downstream induction of matrix metalloproteinase 9 in the pathophysiology of human perinatal white matter damage. *Neuropathol. Exp. Neurol.*, 2010, 69,1116-1129.
23. D. Lapointe, N. Brasseur, J. Cadorette, C. La Madeleine, S. Rodrigue, J.E. van Lier, R. Lecomte. High-resolution PET imaging for in vivo monitoring of tumour response after photodynamic therapy in mice. *J. Nucl. Med.*, 1999, 40, 876-882.
24. C. P. Bleeker-Rovers, F. J. Vos, W. T. A. van der Graaf, J. G. Oyen. Nuclear medicine imaging of infection in cancer patients (with emphasis on FDG-PET). *The Oncologist*, 2011, 16, 980-991.
25. J. Liu, M. Ogawa, T .Sakai, M. Takashima, S. Okazaki, Y. Magata. Differentiation of tumour sensistivity to photodynamic therapy and early evaluation of treatment effect by nuclear medicine techniques. *Ann. Nucl. Med*., 2013, 27, 669-675.
26. N. V. Chandrasekharan, H. Dai, L. T. Roos, N. K. Evanson, J. Tomsik, T. S. Elton, Simmons DL. COX-3, a cyclooxygenase-1 variant inhibited by acetaminophen and other analgesic/antipyretic drugs: Cloning, structure, and expression. *PNAS*, 2002. 99, 13926-13931.
27. I. Morita. Distinct functions of COX-1 and COX-2. *Prostag. Oth. Lipid M.*, 2002, 69, 165-175.
28. K. J. Sales, H. N. Jabbour. Cyclooxygenase enzymes and prostaglandins in pathology of the endometrium. Reproduction, 2003, 126, 559-567.
29. B. J. Tong, J. Tan, L. Tajeda, S. K. Das, J. A. Chapman, R. N. DuBois, S. K. Dey. Heightened expression of cyclooxygenase-2 and peroxisome proliferator-activated receptor in human endometrial adenocarcinoma. *Neoplasia*, 2000, 2, 482-490.
30. G. Ferrandina, F. Legge, F. O. Ranelletti, G. F. Zannoni, N. Maggiano, A. Evangelisti, S. Mancuso, G. Scambia, L. Lauriola. Cyclooxygenase-2 expression in endometrial carcenoma correlation with clinicopathologic parameters and clinical outcome. *Cancer*, 2002, 95, 801-807.
31. K. Watenabe, T. Kawamori, S. Nakatsugi. Inhibitory effect of a prostaglandin E receptor subtype EPI selective antagonist, ONO-8713, on development of azoxymethane-induced aberrant crypt foci in mice. *Cancer Lett.*, 2000, 156, 57-61.
32. H. Sheng, J. Shao, M. K. Washington, R. N. DuBois. Prostaglandin E2 increases growth and motility of colorectal carcinoma cells. J. Biol. Chem., 2001, 276, 18075-18081.
33. S. Narumiya, Y. Sugimoto, F. Ushikubi. Prostanoid receptors: Structures, properties and functions. *Physiol. Rev.*, 1999, 79, 1193-1226.
34. F. Kamachi, H. S. Ban, N. Hirasawa, K. Ohuchi. Inhibition of lipopolysaccharide-induced prostaglandin E2 production and inflammation by the Na+/H+ exchanger inhibitors. *J. Pharmacol. Exp. Ther*., 2007, 321, 345-352.

35. B. W. Henderson, J. M. Donovan. Release of prostaglandin E2 from cells by photodynamic treatment in vitro. *Cancer Res.*, 1989, 49, 6896-6900.
36. L. C. Penning, M. J. Keirse, J. Van Steveninck, T. M. Dubbelman. Ca(2+)-mediated prostaglandin E2 induction reduces haematoporphyrin-derivative-induced cytotoxicity of T24 human bladder transitional carcinoma cells in vitro. *Biochem. J.*, 1993, 292, 237-240.
37. M. T. Foultier, T. Patrice, S. Yactayo, Y. Lajat, F. Resche. Photodynamic treatment of normal endothelial cells or glioma cells in vitro. *Surg. Neurol.*, 1992, 37, 83-88.
38. A. J. Lonigro, M. H. Hagemann, A. H. Stephenson, C. L. Fry. Inhibition of protaglandin synthesis by indomethacin augments the renal vasodilator response to bradykinin in the anesthetized dog. *Circ. Res.*, 1978, 43, 447-455.
39. C. W. Leffler, R. Mirro, L. J. Pharris, M. Shibata. Permissive role of prostacyclin in cerebral vasodilation to hypercapnia in new-born pigs. *Am. J. Physiol.*, 1994, 267, H285-H291.